We are IntechOpen, the world's leading publisher of Open Access books Built by scientists, for scientists

4,800
Open access books available

122,000
International authors and editors

135M
Downloads

Our authors are among the

154
Countries delivered to

TOP 1%
most cited scientists

12.2%
Contributors from top 500 universities

CLARIVATE ANALYTICS BOOK CITATION INDEX INDEXED

WEB OF SCIENCE™

Selection of our books indexed in the Book Citation Index in Web of Science™ Core Collection (BKCI)

Interested in publishing with us?
Contact book.department@intechopen.com

Numbers displayed above are based on latest data collected.
For more information visit www.intechopen.com

Chapter 5

Molecular Magnetism Modeling with Applications in Spin Crossover Compounds

Mihai Dimian and Aurelian Rotaru

Additional information is available at the end of the chapter

http://dx.doi.org/10.5772/64281

Abstract

Molecular magnetic materials have become flourishing fields for research and technological developments due to their novel behavior compared to classical magnetic materials. Molecular magnetism modeling has reached a certain degree of maturity, although several experimental findings are still open problems. This chapter is aimed at providing a general introduction to physical modeling in molecular materials with a special emphasis placed on spin crossover compounds. This presentation includes Ising-type models and their generalizations, such as Wajnflasz and Pick, Bousseksou et al., Zimmermann and König, Sorai and Seki, and Nasser et al., along with their applications to the characterization of phase transition, hysteresis behavior, and thermal relaxations in spin crossover compounds. Recent experimental findings are explained in this context and the relevance of theoretical results for technological applications is also discussed.

Keywords: molecular magnetism, spin crossover compounds, hysteresis, phase transitions, thermal relaxations, modeling and simulations

1. Introduction

Molecular magnetic materials have been in the research spotlight since the current silicon based devices and conventional magnetic storage devices approached their technological and physical limits [1, 2]. In this context, spin crossover (SCO) materials present a special interest due to their unique properties, high versatility, and a wide variety of potential technical applications [3, 4].

The most widely studied SCO materials involve transition metal centers ($3d^4$–$3d^7$) in an octahedral O_h symmetry of ligands. These materials present molecular bistability that can be triggered by various external stimuli such as temperature, pressure, light, magnetic and electric field, and gas absorption [5–16]. The molecular bistability results from the balance between the spin pairing energy and the crystal field that leads to the possibility to populate the 3d orbitals in two different ways characterized by different values of the total spin *S*. These two situations are known in the literature as high-spin (HS) and low-spin (LS) states, respectively. Schematic representation of 3d electron configurations in an octahedral ligand field for Fe (II) complexes in the low-spin ($S = 0$) and the high-spin ($S = 4$) states are presented in **Figure 1**.

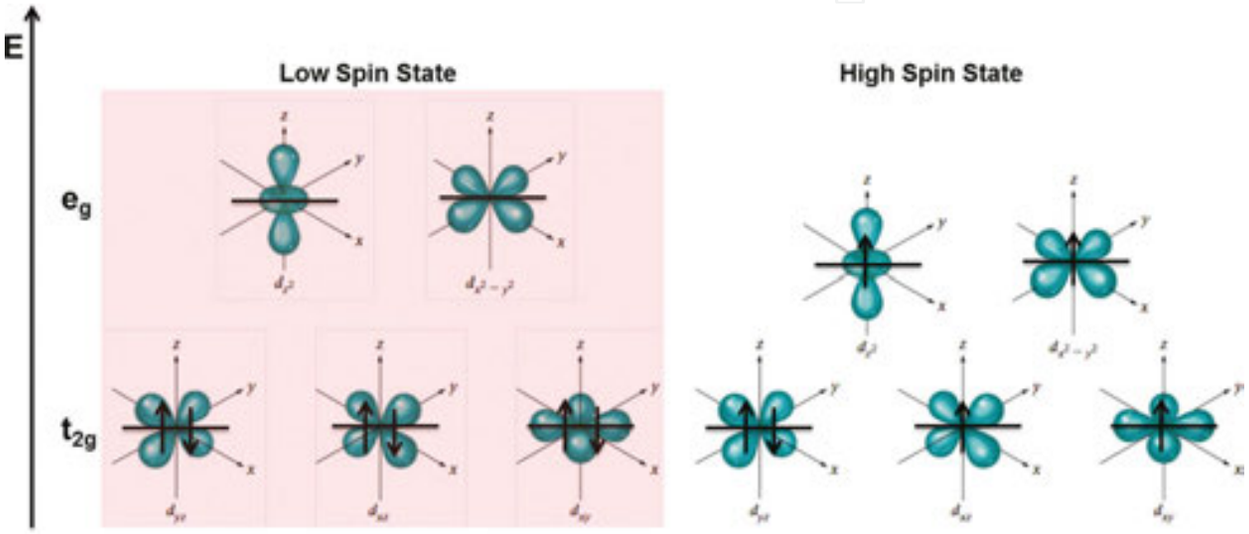

Figure 1. 3d electron configurations in an octahedral ligand field for Fe (II) complexes in the low-spin (S = 0) and the high-spin (S = 4) states, respectively.

The two stable states may feature different magnetic, optical, electrical, and vibrational/structural properties. In the solid state, the structural changes associated to the spin transition propagate in a cooperative manner, which can lead to a hysteretic behavior. From an applicative point of view, SCO materials have been proposed for various technological applications such as recording media, sensors (thermal, pressure, or gas) [17–21], displays [4], molecular switches [22, 23], memristor devices [24–28], or actuators [29, 30].

Molecular magnetism modeling has reached a certain degree of maturity, although several experimental findings are still open problems from theoretical point of view. Here, we provide a review of physical modeling in molecular materials with a special emphasis placed on spin crossover compounds, including Ising-type models and their generalizations, such as Slichter and Drickamer [9], Bousseksou et al. [31], Sorai and Seki [32], and Nasser et al. [33, 34], along with the novel approaches developed in our research group and applied to the characterization of phase transition and hysteresis behavior in molecular magnets [35–41]. Recent experimental findings are explained in this context and the relevance of theoretical results for technological applications is also discussed.

http://dx.doi.org/10.5772/64281

2. Modeling of spin crossover compounds

The theoretical analysis of SCO materials has been developed in two main directions: the molecular approach [31–34, 42–64] and macroscopic approach [9, 65–70], respectively. In the case of the "molecular" models, the interactions between molecules disturb the molecular system and, thus, the statistical thermodynamics can be used to correlate the microscopic parameters of the system with the experiments. The "macroscopic" models use the laws of thermodynamics (phenomenological equations and/or mixture theory) and do not reflect the intrinsic structure of the molecular system.

The first model based on the concept of intermolecular interaction, which was able to qualitatively simulate the spin transition in SCO materials, was proposed by Wajnflasz and Pick in the early 1970s [42, 43]. They assumed that each metal center is a four-level system (two ion beams, each one of them having two spin states) and introduced a fictitious charge to characterize each spin state. The interaction between ionic centers was described by an Ising-like coupling term and the corresponding Hamiltonian was resolved in the mean-field approximation. This model was able to predict both discontinuous and continuous $HS \leftrightarrow LS$ transitions, but its main limitation is related to the nature of the interaction term that is not entirely justified.

The main macroscopic model accounting intermolecular interactions was proposed during the same period by Slichter and Drickamer [9]. This model successfully described the effect of an external applied pressure on the spin transition phenomena and represented the starting point for many macroscopic models attempting to describe the origin of the interactions (atom-phonon coupling, elastic energy, etc.). It is based on the theory of regular solutions assuming a random distribution of molecules in the material. This model was also able to reproduce hysteresis phenomena accompanying discontinuous spin transitions in SCO materials.

In 1974, Sorai and Seki [32] proposed an alternative thermodynamic model by considering that the molecules of the same spin state are organized in spin-like domains, assumed to be independent from each other. The model is similar to the theory of heterophase fluctuations developed by Frenkel and is widely used when the calorimetric data for SCO transition are available. However, their model is rather limited since it is not able to reproduce a hysteretic transition.

In 1977, Zimmermann and König [45] developed a novel model that takes explicitly into account the lattice vibrations. Intramolecular interactions were introduced by using an Ising-like Hamiltonian that was resolved in the Bragg-Williams approximation. The vibration modes were assumed in the Debye approximation, regardless of their intra- or intermolecular origin. The authors also showed a formal equivalence between the two-level models approached in the mean-field approximation and the macroscopic thermodynamic models based on the theory of regular solutions.

The next step was made by Kambara [46] in 1979. This model, based on the theory of the ligand field, assumes that the $HS \leftrightarrow LS$ transition is induced by the Jahn-Teller coupling between the 3d electrons and the local distortion of the base complex Fe.

The link between the thermodynamic model and the experimental results was made by Gutlich et al. [70], changing the input parameters of the Sorai and Seki model.

The first real physical approach of the cooperativity origin was proposed by Onishi and Sugano [65] and Spiering et al. [66], respectively. The authors consider the active molecules, which are susceptible of undergoing a spin transition, as hard spheres inserted into an elastic medium. Indeed, it has been observed that the spin transition was accompanied by a volume change of the SCO molecules. This change will induce a stress field that will propagate in the whole crystallographic lattice due to its elasticity. These spheres were treated as point defects.

A new approach for two-level models was proposed by Bousseksou et al. in the 1990s [31, 71]. They consider that the degeneracy of the two-spin states is much higher than the spin degeneracy ratio. Such degeneracy results from the entropy variation during the spin transition. This new approach allows fitting of the experimental data using input parameters from calorimetric measurements.

Ising-like models can be easily applied, but the nature of the interactions, introduced to describe the cooperativity among the molecules, is not specified. In this regard, in recent years, another series of elastic-like models was proposed. Here, we can distinguish two different approaches. The first approach was proposed by Nishino et al. [58] and Enachescu et al. [60], where they consider that the interactions are elastic in their nature, i.e., the molecules are interacting via the change of the molecular volume. The second approach is proposed by Nasser et al. [33, 34], which is known in the literature as "atom-phonon coupling" (APC) model. The basic idea of the APC model is that the elastic constants that characterize the coupling between neighboring molecules depend on their spin state. This model has proven its complexity, being able to reproduce a wide range of characteristic behaviors to spin transition compounds [35–37, 39, 41, 72, 73].

2.1. Slichter and Drickamer model

The model proposed by Slichter and Drickamer assumes a mixture of both HS and LS constituents in the solid. If we denote by n_{LS} and n_{HS} the associated mole fractions of the LS and HS states, respectively, the free enthalpy of the interacting ions centers can be then expressed as

$$G = n_{LS}G_{LS} + n_{HS}G_{HS} - TS_{mix} + \Gamma n_{HS}n_{LS}\,, \tag{1}$$

where Γ is the term of intermolecular interaction and S_{mix} is the mixed entropy of an ideal mixing solution of LS and HS molecules, given by $S_{mix} = -R(n_{LS} \ln n_{LS} + n_{HS} \ln n_{HS})$ with R being the gas constant (= 8.3144598(48) J K^{-1} mol^{-1}). If G_{LS} is considered as origin level for energies, then $G_{LS} = 0$, while $G_{HS} = \Delta G = \Delta H - T\Delta S$, with ΔH and ΔS being the entropy and the enthalpy variations, respectively, during the spin transition. As a consequence, the free enthalpy can be written as follows:

$$G = n_{HS}\Delta H - \Gamma n_{HS}(1 - n_{HS}) + RT\left[(1 - n_{HS})\ln(1 - n_{HS}) + n_{HS}\ln n_{HS} + n_{HS}\frac{\Delta S}{R}\right]. \quad (2)$$

The equilibrium condition of the system, $\left(\frac{\partial G}{\partial n_{\mathrm{HS}}}\right)_{T,p}=0$, leads to the implicit expression of n_{HS} as a function on T

$$T = \frac{\Delta H + \Gamma(1-2n_{HS})}{R\ln\left(\frac{1-n_{HS}}{n_{HS}}\right)+\Delta S}. \quad (3)$$

The solution of Eq. (3) for HS molar fraction as a function of temperature is plotted in **Figure 2**, for several values of intermolecular interaction constants considering variations of enthalpy and entropy specific to Fe(II) SCO compounds.

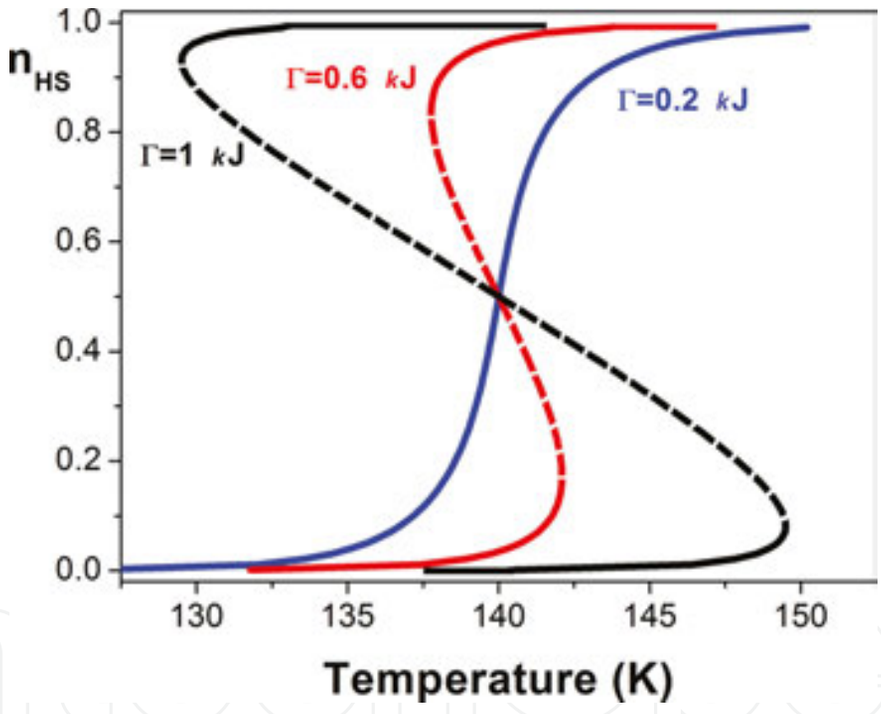

Figure 2. Thermal variations of the HS molar fraction for three selected values of the intermolecular interaction constant Γ = 0.2, 0.6, and 1 kJ. The following values have been used for the enthalpy and entropy variations: ΔH = 7 kJmol^{-1} and ΔS = 50 JK^{-1}mol^{-1}.

2.2. Sorai and Seki model

The model proposed by Sorai and Seki considers that LS and HS molecules are not randomly distributed but organized in spin-like domains, i.e., regions of molecules having the same spin state. Thus, the SCO system consists of several noninteractive domains having the same

number of molecules (n) and transition temperature around a critical temperature T_c (=$\Delta H/\Delta S$). The equilibrium condition leads to the following explicit expression of n_{HS} as a function on T:

$$n_{HS} = \frac{1}{1+exp\left(\frac{n\Delta H}{R}\left(\frac{1}{T}-\frac{1}{T_c}\right)\right)}. \tag{4}$$

For single-molecule domain, the solution is the same with the one found from Eq. (3) in the case of noninteractive particles. The introduction of spin-like domains in the model leads to a better control of the spin transition path, as reflected by **Figure 3(a)**, where the thermal variation of HS molar fraction is plotted for various numbers of molecules included in a spin-like domain. The Sorai and Saki model is widely used in the case when the calorimetric data of the SCO compounds are available. From calorimetric measurements, such as molar heat capacity at constant pressure as a function of temperature, $C_p = f(T)$, the number of molecules per domain can be calculated by using the following formula:

$$n = \frac{4RT_c^2}{(\Delta H)^2}\left(C_p(T_c) - \frac{1}{2}\left(C_{LS}(T_c) + C_{HS}(T_c)\right)\right), \tag{5}$$

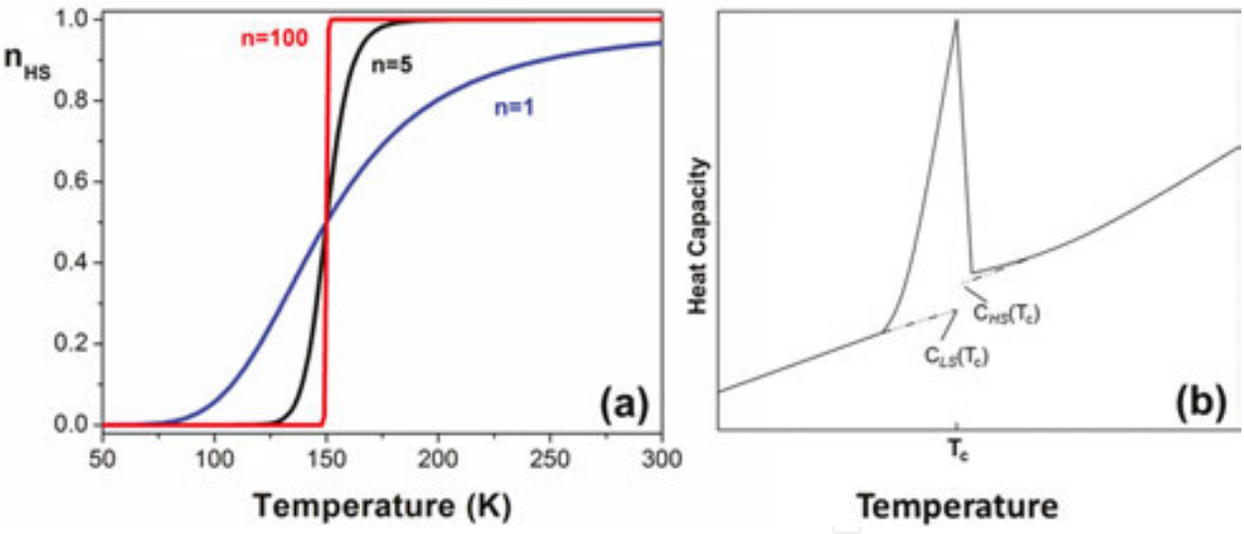

Figure 3. (a) Thermal variations of the HS molar fraction for three selected values of the number of molecules per domain n = 1, 5, and 100. The following values have been used for the enthalpy variations and critical temperature: ΔH = 7 kJmol^{-1} and T_c = 150 K and (b) typical heat capacity variation as a function of temperature and definitions of C_{LS} and C_{HS}.

where C_{LS} and C_{HS} are defined as "normal" heat capacities of LS and HS states as described in **Figure 3(b)**. Although n is considered a relevant measure of the spin cooperativity during phase transition, the lack of interaction between domains leads to an important limitation of Sorai and Seki model, since it is not able to reproduce hysteretic transition.

http://dx.doi.org/10.5772/64281

2.3. Ising-like model

The model proposed by Varret research group [31] has taken into account the degenerate energy levels and it was successfully used to describe both static and dynamic properties of SCO compounds under different external stimuli such as temperature, pressure, magnetic, and electric fields [74, 75]. The model Ising-like Hamiltonian can be written as follows:

$$H = \frac{1}{2}\sum_i (\Delta - k_B T \ln g)\,\hat{\sigma}_i - \sum_{\langle i,j\rangle} J_{ij}\hat{\sigma}_i\hat{\sigma}_j - L\langle\hat{\sigma}\rangle\sum_i \hat{\sigma}_i\,, \tag{6}$$

where $\hat{\sigma}_i$ is the fictitious spin operator associated to molecule i having the eigenvalues +1 (when the molecule is in the HS state) and −1 (when the molecule is in the LS state), Δ is the internal energy gap between the HS and LS states, k_B is the Boltzmann constant (= 1.38064852(79) × 10^{-23} J K^{-1}), g is the degeneracy ratio between HS and LS energy levels (>1), J_{ij} stands for the short-range interaction parameter representing the cooperative interaction that only exists between the nearest-neighboring pairs (J_{ij} includes the nearest-neighbors number), i, j denotes the fact that the sum is only made over the nearest-neighbors pairs, and L stands for long-range interaction parameter that is expressed here in a mean-field approach with $\langle\hat{\sigma}\rangle$ being the average fictitious spin.

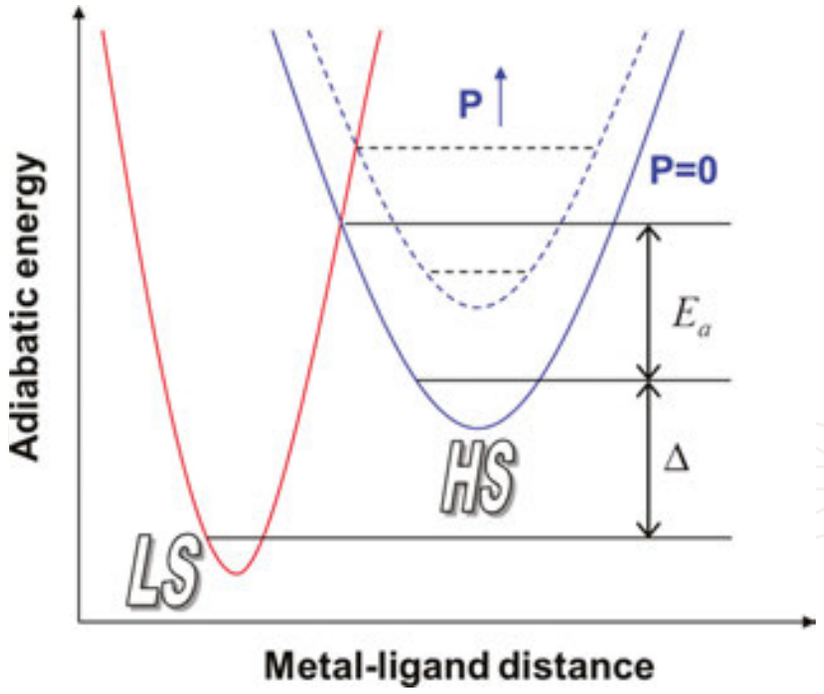

Figure 4. Pressure effect on the configuration diagram.

Hamiltonian (6) takes into account both short- and long-range interactions, while spin and energy degeneracies are considered as a temperature-dependent effective field $(\Delta - k_B T \ln g)/2$ acting on each spin. In noninteractive system, the critical temperature T_{0c}, at which

$n_{HS} = n_{LS} = 0.5$, corresponds to a zero effective field and, consequently, it is related to the energy gap and degeneracy ratio as follows: $T_{0c} = \Delta/k_B \ln g$. Let us now denote by T_{Ic}, the critical temperature at which phase transition happens in purely ferromagnetic Ising systems formed by the second term in Hamiltonian (6) with J_{ij} positive. If the critical temperature in purely Ising model is smaller than the critical temperature in noninteractive model ($T_{Ic} < T_{0c}$), then a gradual spin transition from LS to HS takes place by increasing the temperature. Otherwise, the spin transition is discontinuous and is associated to a first-order phase transition. The addition of long-range interactions, the last term in Hamiltonian (6), can significantly change the system behavior.

For example, purely one-dimensional Ising systems generate no phase transition, and, consequently, the addition of degeneracy term does not contribute to the appearance of phase transition (since T_{0c} is larger than $T_{Ic} = 0$). However, when long-range interactions are introduced, various types of spin transition are possible, including multiple-step transitions and hysteretic transitions [76–79].

Next, we will discuss how this model can be adapted and applied to analyze the effects of external pressure on SCO behavior. It was experimentally observed that variations of the external pressure can give rise to transitions between HS state and LS state. This process, governed by entropy, can be better understood by assuming two potential wells, each representing a possible spin state as a function of a configuration coordinate (metal-ligand distance), as represented in **Figure 4**. The application of an external pressure decreases intermolecular distances and, by consequence, the metal-ligand distances. Since the ligand field is inversely proportional to the metal-ligand distance (to the sixth power), the application of external pressure has a similar effect as the substitution of ligands to the central metal, so the potential wells can move vertically and horizontally by changing the metastable state [9, 31, 43, 74, 80].

The energy gap dependence on the pressure can be expressed as:

$$\Delta(p) = \Delta(p = 0) + p\delta V\,, \tag{7}$$

where δV is the volume variation of the SCO molecules during the spin transition phenomenon and p is the externally applied pressure. By considering the mean-field approach, the behavior of the system described by Eq. (6) coupled with Eq. (7) can be approximated by behavior of a noninteracting system of spins with one-site Hamiltonian H_{mf} written as

$$H_{mf} = \frac{\Delta(p) - k_B T \ln g}{2}\hat{\sigma} - (qJ + L)\hat{\sigma} < \hat{\sigma} > \,, \tag{8}$$

where q is the number of nearest neighbors. The average fictitious spin $\langle\hat{\sigma}\rangle$ is also known as "fictitious magnetization" and will be further denoted by m. The resulting mean-field equation m has the following form:

http://dx.doi.org/10.5772/64281

$$m = \tanh\left(\frac{(qJ+L)m}{k_BT} + \frac{k_BT\ln g - \Delta(p)}{2k_BT}\right). \tag{9}$$

For the sake of simplicity, in the following calculations we use several normalizations, namely, the energy gap $\Delta = \Delta(p)/k_B$, the interaction parameter $\Gamma = (qJ + L)/k_B$ (which includes both short- and long-range interaction), and the volume variation $\alpha = \delta V \cdot 10^{-5}/k_B$ (where the factor 10^{-5} stands for the conversion of the pressure units from *pascal* to *bar*). Sample results for hysteretic transitions driven by temperature and pressure variations are presented in **Figure 5**, for Δ = 1000K, ln g = 7, Γ = 400K, α = 4K/bar, where the HS fraction n_{HS} is simply related to the fictitious magnetization m by $n_{HS} = (1 + m)/2$.

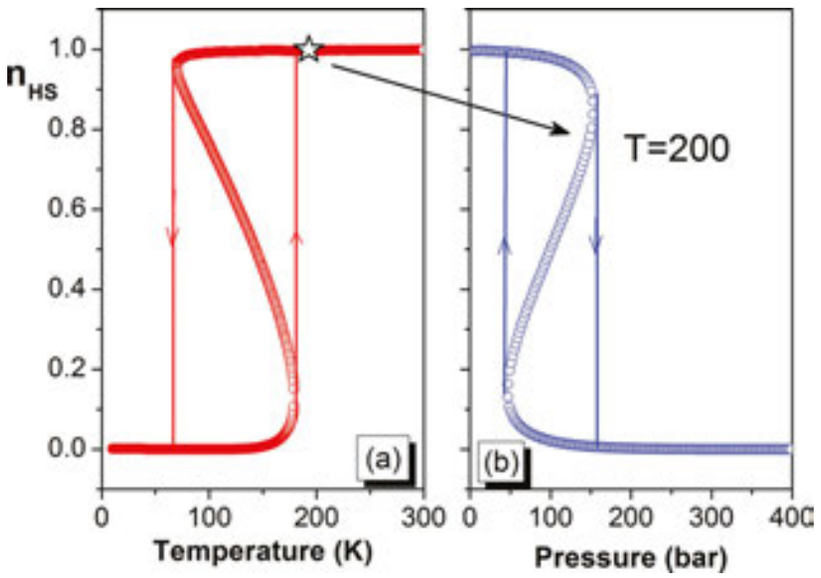

Figure 5. (a) Thermal hysteresis loop computed for pressure p = 1 bar and (b) pressure hysteretic loop for T = 200K. The normalized parameters used in these calculations are Δ = 1000K, ln g = 7, Γ = 400K, α = 4K/bar.

By increasing the applied pressure, the switching temperatures will shift to higher values, thus making it possible to control the system switching temperature by external inputs. However, the width of hysteretic loop is reduced by this action and, at some critical value of the applied pressure, the SCO system will lose its cooperativity, i.e., the hysteretic loop disappears leading to a continuous spin transition. The 3D phase diagrams' (T, p, n_{HS}) coordinates are presented in **Figure 6**, for a system with noninteractive molecule (left) and for a cooperative system with interaction constant Γ = 400K (right). The other parameters are the same as in the previous discussion Δ = 1000K, ln g = 7, α = 4K/bar. In order to separate the hysteretic part from nonhysteretic part of the phase diagram, let us observe that the transition temperatures (pressures) can be obtained as maxima and minima of the temperature (pressure) as a function of n_{HS}, or, equivalently, as a function of m. The expression of temperature in terms of m can be obtained by inverting Eq. (9) as follows:

$$T = \frac{\Delta(0) + \alpha p - 2\Gamma m}{\ln g - \ln\left(\frac{1+m}{1-m}\right)} \quad . \tag{10}$$

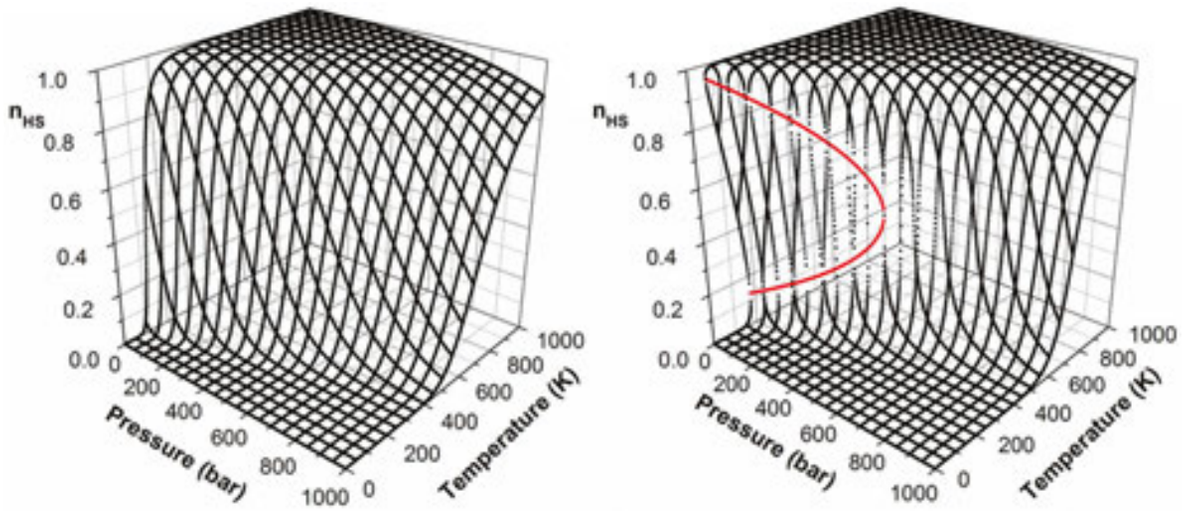

Figure 6. The 3D phase diagram for a system of noninteractive spins (left) and for a cooperative system with Γ = 400K (right). The red curve from the right image represents the spinodal curve. The normalized parameters used in these calculations are Δ = 1000K, ln g = 7, α = 4K/bar.

In order to find the extrema of T as a function of m, the derivative dT/dm is set to be zero, leading to the following algebraic equation:

$$\frac{1}{2}\left(m^2 - 1\right)\left(\ln\left(\frac{1+m}{1-m}\right) - \ln g\right) + 2m = \frac{1}{\Gamma}\left(\Delta(0) + \alpha p\right) \quad . \tag{11}$$

By varying pressure, the solution of this equation describes in (T, p, n_{HS}) space, a critical curve, also known as spinodal curve, which delimits the hysteretic part of the phase diagram from the nonhysteretic one, as presented from **Figure 6**.

2.4. Atom-phonon coupling model

Atom-phonon coupling model has been proposed by Nasser et al. [33, 34], with the aim to overcome some deficiencies of Ising-like models concerning the origin of the interaction parameter. Moreover, APC model is taking into account the results of Sorai and Seki, regarding the dependence of the Debye temperature as a function of the HS fraction [32]. In Sorai and Seki model, the importance of the contribution of phonons in the transition phenomenon is emphasized. A similar approach has been also discussed by other authors in Refs. [81, 82].

Although the APC model was initially proposed for the characterization of the thermal behavior of the SCO compounds, its applicability has been extended afterwards in order to describe the process of photoexcitation observed at low temperature light-induced excited spin

http://dx.doi.org/10.5772/64281

state trapping (LIESST) [37, 39, 41], the relaxation process of the photo-excited metastable states and light-induced thermal hysteresis (LITH) [35], as well as the effect of externally applied pressure [36, 37].

In the APC model, the spin crossover molecules are modeled as atoms linked by springs, i.e., the intramolecular vibrations are not taken into account. As in the Ising-like model, a fictitious spin $\hat{\sigma}_i$ is associated to each molecule that can take two eigenvalues: −1, corresponding to the fundamental level LS, and +1, corresponding to the HS level. According to the spin state of the neighbor atoms, three values of the elastic constants taken into account are denoted by λ when both molecules are in the LS state, ν when both molecules are in the HS state, and μ when one atom is in the LS state and the other is in the HS state. From Brillouin and Mossbauer spectroscopy [83, 84] data, it was shown that the elastic constants are smaller in the HS state than in the LS state. Thus, at a given temperature, phonons promote the HS state while the HS-LS energy gap promotes the LS state, leading to an interesting competition between two mechanisms. Consequently, in the APC model, it is considered as $\nu < \mu < \lambda$.

The APC Hamiltonian is given by the sum of two contributions: electronic and vibrational:

$$H = H_{spin} + H_{ph} = \left(\sum_{i=1}^{N} \frac{\Delta}{2} \hat{\sigma}_i \right) + \left(E_c + E_p \right) \ , \tag{12}$$

where N is the number of spins in the system, Δ is the energy gap between these LS and HS states, and E_c and E_p are the kinetic energy and the potential energy of the system, respectively. The kinetic energy is simply written as:

$$E_c = \sum_{i=1}^{N} \frac{p_i^2}{2m_a} \ , \tag{13}$$

where i is the impulse of atom and m_a is the mass of the SCO atom. For a chain of N atoms, the potential energy can be written as:

$$E_p = \sum_{i=1}^{N} \frac{1}{2} e_{i,i+1} (u_{i+1} - u_i)^2 \ , \tag{14}$$

where u_i is the longitudinal displacement of the ith atom from its equilibrium position that is assumed to be independent of the electronic state of the atom i and its neighbors and $e_{i,i+1}$ is the elastic constant between the ith atom and the $(i+1)$th atom. By taking into account the previous discussion related to the state-dependent elastic constants, a concise formula can be obtained for $e_{i,i+1}$ in terms of λ, μ, ν and the fictitious neighboring spins $\hat{\sigma}_i$ and $\hat{\sigma}_{i+1}$:

$$e_{i,i+1} = \frac{\lambda + 2\mu + \nu}{4} + \frac{\nu - \lambda}{4} (\hat{\sigma}_i + \hat{\sigma}_{i+1}) + \frac{\lambda - 2\mu + \nu}{4} \hat{\sigma}_i \hat{\sigma}_{i+1} \ . \tag{15}$$

The periodic boundary conditions are considered, as apparent from **Figure 7**, so $\hat{\sigma}_{N+1}$ is actually $\hat{\sigma}_1$. By plugging Eq. (15) in Eq. (14), the potential energy can be rewritten as the sum of three terms V_0, V_1, and V_2 where:

$$V_0 = \sum_{i=1}^{N} \frac{\lambda + 2\mu + \nu}{8} (u_{i+1} - u_i)^2, \tag{16}$$

$$V_1 = \sum_{i=1}^{N} \frac{\nu - \lambda}{8} \left[(u_i - u_{i-1})^2 + (u_{i+1} - u_i)^2 \right] \sigma_i, \tag{17}$$

$$V_2 = \sum_{i=1}^{N} \frac{\lambda - 2\mu + \nu}{8} (u_{i+1} - u_i)^2 \sigma_i \sigma_{i+1}. \tag{18}$$

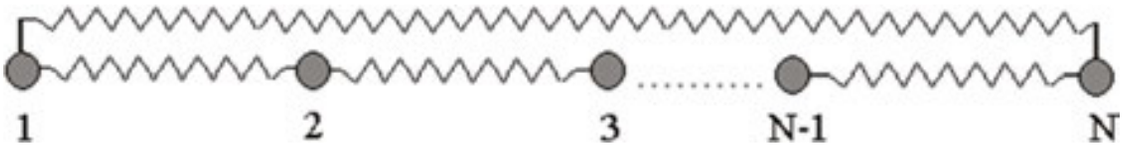

Figure 7. Chain of atoms bound together by springs with periodic boundary conditions.

It is apparent from Eq. (17) that V_1 has the expression of Zeeman-like energy, each spin $\hat{\sigma}_i$ being subject to an effective field h_i given by:

$$h_i = \frac{\nu - \lambda}{8} \left[(u_i - u_{i-1})^2 + (u_{i+1} - u_i)^2 \right]. \tag{19}$$

where $\nu < \lambda$ in this field promotes the HS state (eigenvalue +1). It is apparent from Eq. (18) that V_2 has the expression of exchange-like energy, so an effective exchange parameter $J_{i,i+1}$ can be defined as follows:

$$J_{i,i+1} = \frac{\lambda - 2\mu + \nu}{8} (u_{i+1} - u_i)^2. \tag{20}$$

The sign of exchange constant depends on the relation between μ and $(\nu + \lambda)/2$, and the exchange term disappears when the elastic constant for HS-LS case is the average of the elastic constants for LS-LS and HS-HS states, i.e., $\mu = (\nu + \lambda)/2$.

In the mean-field approximation, the elastic constant $e_{i,i+1}$ can be replaced by an effective elastic constant K that does not depends on site i. Thus, the effective field h_i generated by the phonons is uniform throughout the chain and the effective exchange parameter $J_{i,i+1}$ is the same for each pair of neighboring spins. The system can be studied by using transfer-matrix method [85], and the resulting mean value for the phonon Hamiltonian can be expressed as follows:

http://dx.doi.org/10.5772/64281

$$\left\langle H_{phon}(K)\right\rangle_T = \frac{\hbar\omega_M(\lambda)}{2}\sqrt{\frac{K}{\lambda}}\cdot\sum_{i=1}^{N}\left|\sin\frac{i\pi}{N}\right|\coth\left(\frac{\hbar\omega_M(\lambda)}{2k_BT}\sqrt{\frac{K}{\lambda}}\left|\sin\frac{i\pi}{N}\right|\right), \tag{21}$$

where $\hbar$ is the reduced Planck constant (= 1.054571800(13) × 10^{-34} J s^{-1}) and $\omega_M(\lambda)$ is the maximum phonon angular frequency for a periodic chain with an elastic constant λ ($\omega_M(\lambda)=2\sqrt{\lambda/m_a}$). The effective elastic constant K can be obtained by applying the variational method [86]:

$$K = \frac{2\mu+\lambda+\nu}{4} + 4h_0\cdot m + 2J_0\cdot s\ , \tag{22}$$

where $h_0=\frac{\nu-\lambda}{8}$, $J_0=\frac{\lambda-2\mu+\nu}{8}$ and $m=\langle\hat{\sigma}_i\rangle$, $s=\langle\hat{\sigma}_i\hat{\sigma}_{i+1}\rangle$ are the two-order parameters known as the fictitious magnetization and correlation parameter, respectively. From the transfer matrix method [85], the following system of two nonlinear equations is obtained for the two unknown m and s:

$$\begin{cases} m = \dfrac{\exp\left(J/k_BT\right)\sinh\left(h_g/k_BT\right)}{\sqrt{\exp\left(2J/k_BT\right)\sinh^2\left(h_g/k_BT\right)+\exp\left(-2J/k_BT\right)}} \\ s = 1-\dfrac{2m^2\exp(-4J/k_BT)}{\sinh\left(h_g/k_BT\right)\left(m\cosh\left(h_g/k_BT\right)+\sinh\left(h_g/k_BT\right)\right)} \end{cases}, \tag{23}$$

where the implicit dependencies of the right-hand side terms on m and s are presented in h_g and J that depend on K (see also Eqs. (21) and (22)) as follows:

$$\begin{cases} h_g = -\dfrac{\Delta}{2} - \dfrac{2h_0}{K}\dfrac{\left\langle H_{phon}(K)\right\rangle_T}{N} + k_BT\dfrac{\ln g}{2} \\ J = -\dfrac{J_0}{K}\dfrac{\left\langle H_{phon}(K)\right\rangle_T}{N} \end{cases}, \tag{24}$$

where g is the degeneracy factor equal to the ratio between the degeneracy of the HS energy level and the degeneracy of the LS energy level. In conclusion, once the SCO parameters are given, namely, Δ, g, N, h_0, J_0, λ, m_a, the formula (23) contains two self-consistent equations for m and s that can be solved for each value of the temperature T.

Since the HS fraction n_{HS} is simply related to the fictitious magnetization m by the formula $n_{HS}=(1+m)/2$, the dependence of n_{HS} on temperature is thus obtained. For the sake of simplicity in the following calculations, we use several normalizations, namely:

- the reduced temperature $t_r = \frac{k_B T}{\hbar \omega_M(\lambda)}$;
- the dimensionless electronic excitation energy $\delta = \frac{\Delta}{\hbar \omega_M(\lambda)}$;
- the elastic constant ratio $x = \frac{\nu}{\lambda}$; and
- the dimensionless parameter y defined by $\mu = \frac{\lambda + \nu}{2} + \frac{\lambda - \nu}{2} y$.

The dimensionless parameter x is a measure of the interaction intensity in the system, a small value of x implying strong interactions in the system. The dimensionless parameter y shows how close is μ to λ as compared to ν, a positive value of y implying that μ is closer to λ while a negative value of y implying that μ is closer to ν. It is apparent that for $y = 0$, μ is the mean value of λ and ν. By using this normalization and the property of the above algebraic system that uses only ratios of elastic constants to λ, the 8-parameter problem is now reduced to 6-parameter problem: 4 normalized parameters presented above along with the number of atoms N and degeneracy ratio g. An example of hysteretic transition for a SCO chain driven by temperature, computed in the APC model, is plotted in **Figure 8**.

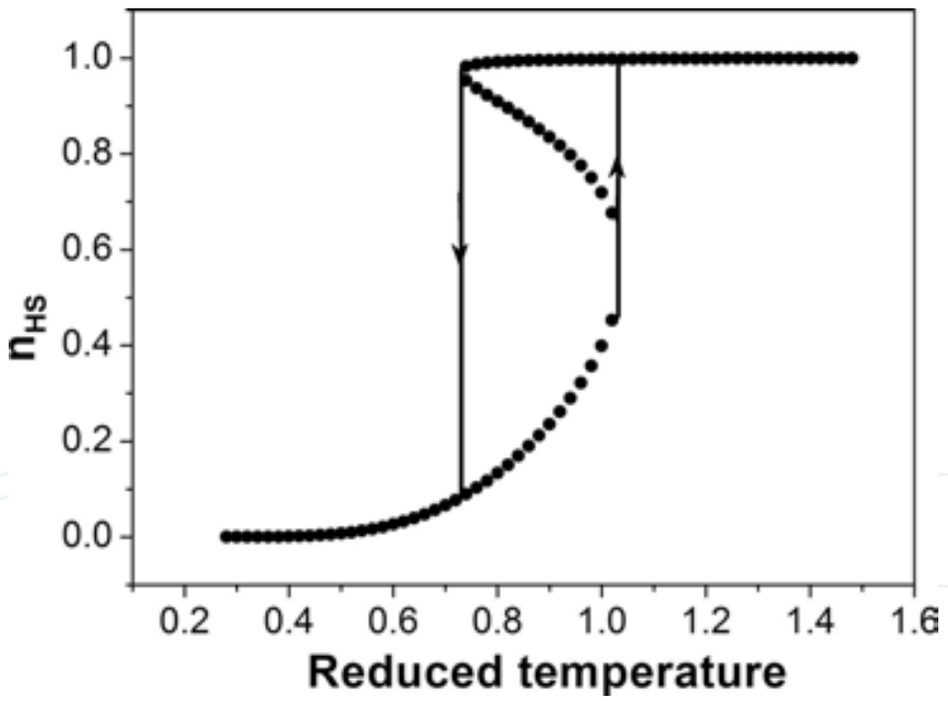

Figure 8. Thermal hysteresis loop for a SCO chain computed in the APC model. The reduced parameters used in these calculations are $x = 0.2$, $y = 0$, $\delta = 0.606$, while $\ln g = 5$, $N = 2000$.

The size effect plays a very important role in applications such as information storage technology. The problem is to estimate the minimum size for which the system still maintains its hysteretic properties. An important advantage of the APC model is that the system size appears naturally in the Hamiltonian, allowing a direct analysis of the size effect, i.e., the dependence

http://dx.doi.org/10.5772/64281

of the hysteresis loop width on the number of atoms N. Since the intermolecular interactions also play a crucial role in the width of hysteresis loop, we present in **Figure 9**, the variation of hysteresis loop width with the system size for two values of the elastic constant ratio x. As expected, the hysteretic loop is wider when stronger interactions are present in the system (i.e., x is smaller), but it is interesting to observe that critical system size for hysteretic behavior is also decreasing with the increase in the interaction strength. A saturation phenomenon in hysteretic loop width is also observed with the increase in system size. A more detailed analysis of this important topic can be found in Refs. [36, 80].

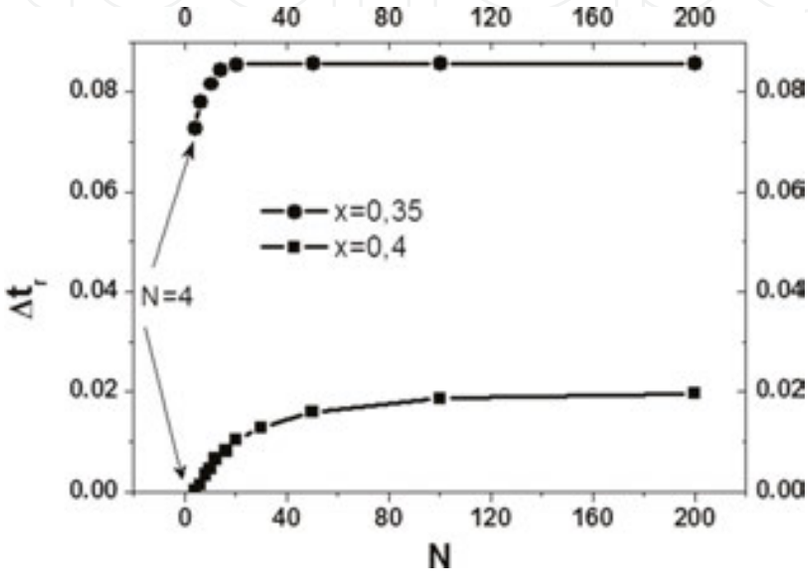

Figure 9. Size dependence of the SCO hysteresis width computed in the APC model for two different values of the elastic constant ratio x. The other reduced parameters used in these calculations are $y = 0$, $\delta = 0.606$, while $\ln g = 5$.

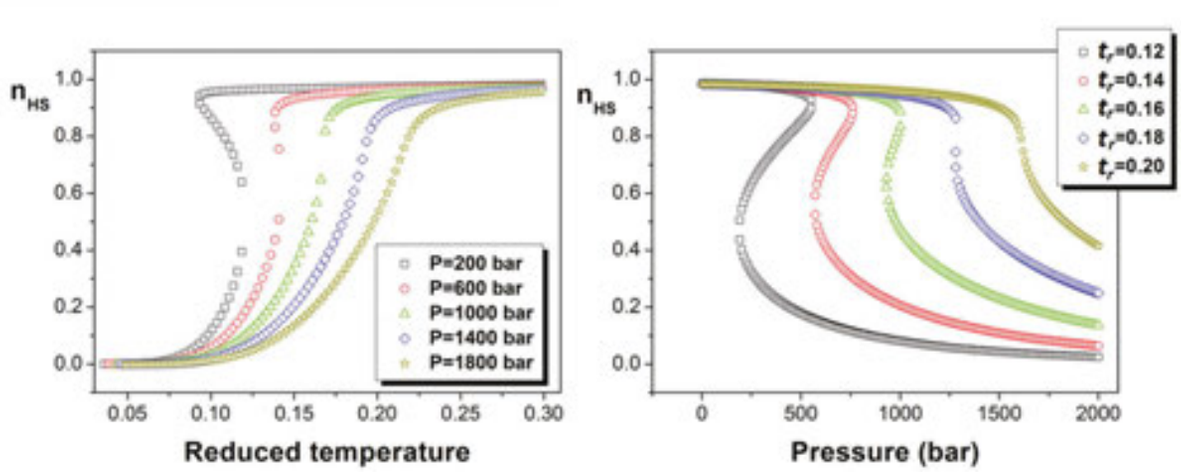

Figure 10. (Left) Thermally driven transitions computed for selected values of pressure indicated in the figure. (Right) Pressure-driven transitions computed for selected values of the reduced temperature indicated in the figure. The parameters used in these calculations are $x = 0.4$, $y = 0.8$, $\delta_0 = 0.525$, $\alpha = 10^{-4}\text{bar}^{-1}$, $\ln g = 5$, and $N = 2000$.

Next, we will focus on the *pressure effect* on the spin transition driven by temperature as well as on the *temperature effect* on the spin transition driven by external pressure. Based on several results obtained by Raman spectroscopy, the vibrational properties of SCO systems seem to remain stable when external pressure is applied [84]. Thus, we can assume that the ratio of the elastic constants does not depend on pressure and the pressure effect will be accounted only in the energy gap: $\Delta_p = \Delta_0 + p\delta V$, as it was also considered in the Ising-like model. By substituting the new expression for the energy gap in Eq. (28), the solution for the fictitious magnetization will be dependent on the external pressure. The dimensionless electronic excitation energy will be now defined as $\delta_0 = \Delta_0/\hbar\omega_M(\lambda)$ and a normalized volume variation is introduced as $\alpha = \delta V \cdot 10^{-5}/\hbar\omega_M(\lambda)$ (where the factor 10^{-5} stands for the conversion of the pressure units from *pascal* to *bar*). Sample results for spin transitions driven by temperature and pressure variations are presented in **Figure 10**, for $x = 0.4$, $y = 0.8$, $\delta_0 = 0.525$, $\alpha = 10^{-4}\text{bar}^{-1}$, $\ln g = 5$, and $N = 2000$.

It should be noted that the pressure hysteresis loops computed in the APC model present an elongation at high pressure, in good agreements with the experimental observations [87]. However, in some coordination compounds, the electronic transitions do not always arise from a simple configuration. The external pressure can also induce a crystallographic phase transition, giving rise to an unusual behavior, such as the increase of the hysteretic loop width with the increase in the applied pressure [16].

2.4.1. Relaxation process of the photo-excited HS metastable states at low temperature

The bistable nature of spin crossover materials coupled to their sensitivity to light irradiation is of particular interest for the development of data-recording media. At low temperatures (typically below 40 K), the system can be switched from the ground low-spin state to the metastable high-spin state using appropriate wavelengths known as light-induced excited spin state trapping effect [6]. The relaxation from high-spin state to low-spin state (HS → LS) appears if, after photoexcitation, the light is switched off.

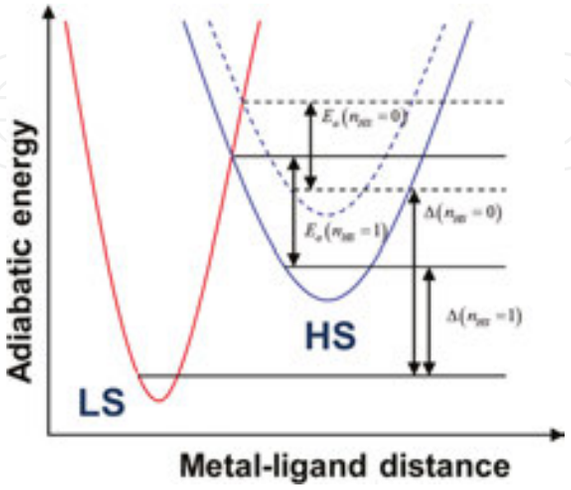

Figure 11. Configuration diagram of a spin crossover molecule showing the energy barrier variation.

At low temperature (<30 K), the relaxation process occurs by tunneling, while at higher temperature (>40 K), this process is thermally activated and consequently it is very fast at room temperature, where the life time is in the order of 10^{-8} to 10^{-6} *s* [88]. The relaxation process from high-spin state to low-spin state was studied in detail by Andreas Hauser and the Mainz group [88–90]. This analysis was based on the energy barrier properties of the state (HS) and led to the understanding of the main properties of the SCO cooperative relaxation. As illustrated in **Figure 11**, the energy gap Δ is increasing and the activation energy E_a is decreasing with the decrease of the molar high-spin fraction n_{HS}. Consequently, the relaxation (HS → LS) becomes faster with the decrease of n_{HS} leading to a self-accelerating process.

The expression of the relaxation rate, K_{HL}, was introduced by Hauser, on experimental and theoretical bases, by considering a linear dependence of the barrier energy with n_{HS}. In APC model, a more realistic formula for the energy barrier was derived and used to describe the relaxation process. Thus, the activation energy can be expressed as follows:

$$E_a = E_0 - E_{HS} = E_0 - \frac{\Delta}{2} - \frac{2h_0}{K}\frac{\left\langle H_{phon}(K)\right\rangle_T}{N} \quad , \tag{25}$$

where E_0 is the level of the energetic barrier. In the thermal activation regime, the relaxation rate is given by the standard relation:

$$K_{HL}(T, n_{HS}) = k_\infty \exp\left(-\frac{E_a}{k_B T}\right) \quad , \tag{26}$$

where k_∞ is the high-temperature relaxation rate (associated to vibrational frequencies). The variation in time of the high-spin fraction is given by the master equation

$$\frac{dn_{HS}}{dt} = -n_{HS} K_{HL}\left(T, n_{HS}\right) \quad , \tag{27}$$

where $K_{HL}(T, n)$ is given by Eq. (26) in which E_a is given by Eq. (25).

Sample results for the SCO relaxation curves calculated by using the above formulas derived in the APC model are presented in **Figure 12**, for several values of the interaction parameter x, and in **Figure 13**, for several values of the temperature at which relaxation process occurs. The values for the reduced parameters of the system (introduced above) used in these calculations are given in the figures' captions. In addition, a new normalized parameter is introduced and denoted by A, which is defined by $A = E_0/\hbar\omega_M(\lambda)$.

As can be seen from **Figure 12**, the relaxation process is getting slower when the interaction between the molecules is getting stronger (i.e., smaller values of x). It is important to observe the sigmoidal shape of the relaxation curve which is in good agreement with the experimental data. Moreover, APC model also resolves one of the weaknesses of Hauser model, which was

not able to reproduce the so-called "tail-effect," i.e., the slow-relaxation effect observed for small values of molar high-spin fraction. Since these results were derived in the framework of classical Arrhenius-type activation, the relaxation process of the photo-excited metastable states can also be analyzed by using the Arrhenius representation $\ln(K_{HL}) = f(n_{HS})$, as shown in **Figure 14**. Here, the shape of the resulting Arrhenius diagram shows two slopes, in good agreement with the experimental data, unlike the Hauser model, where the Arrhenius diagram is a straight line [91].

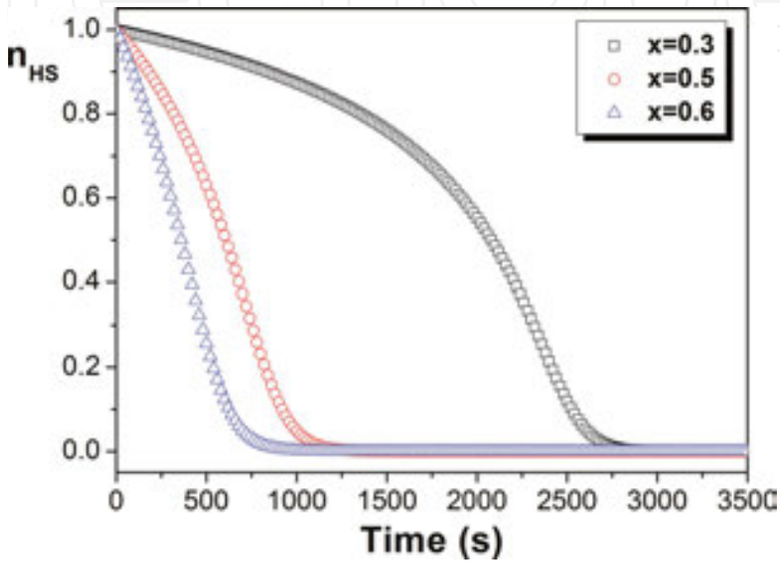

Figure 12. Relaxation curves recorded in dark for selected values of interaction parameter x. The parameters used in the calculations are $y = 0$, $\delta_0 = 0.6$, $t_r = 0.03$, $\ln g = 5$, $N = 2000$, $A = 0.8$, and $k_\infty = 100$.

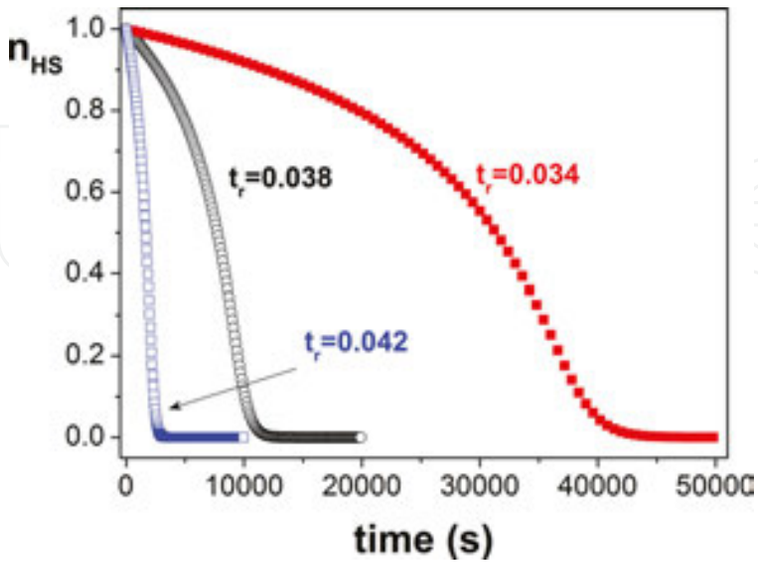

Figure 13. Relaxation curves recorded in dark for selected values of the reduced temperature t_r at which relaxation process occurs. Parameters used in the calculations are $y = 0$, $\delta_0 = 0.6$, $x = 0.2$, $\ln g = 5$, $N = 2000$, $A = 0.8$, $k_\infty = 100$.

http://dx.doi.org/10.5772/64281

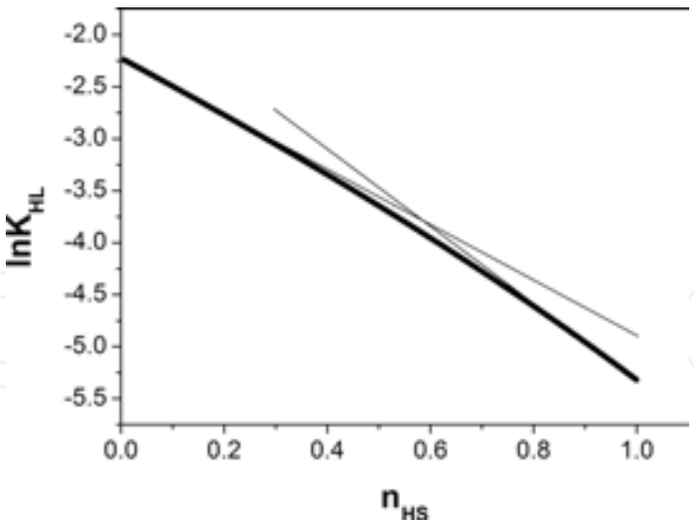

Figure 14. Arrhenius diagram of the relaxation process in SCO compounds in APC model.

Since we focused on thermally activated relaxations, it is apparent that the relaxation process speeds up with the increase of temperature, as shown in **Figure 13**, as well. In practice, the switch from HS state to LS state can be achieved either by direct nonradiative relaxation or by the reverse LIESST effect when the samples is irradiating in the HS state absorption band [8].

2.4.2. Light-induced thermal hysteresis

Experiments under permanent light irradiation illustrate the competition between the *noncooperative* photoexcitation (generating LS → HS transitions) and the cooperative relaxations (HS → LS) that are thermally activated. This competition leads to hysteretic transition known as light-induced thermal hysteresis. Light-induced thermal hysteresis was discovered almost simultaneously by the groups of F. Varret from Versailles [88] and O. Kahn from Bordeaux [92], respectively.

The LITH explanation given by Varret's group goes as follows: at low temperatures, the metastable HS states are populated by LIESST effect; by increasing the temperature, while maintaining the light irradiation, thermally activated relaxations (HS → LS transitions) get stronger leading the system into a metastable state where thermal relaxations balance the LIESST effect. Quantitatively, this situation can be expressed by introducing in relaxation Eq. (27) an additional term accounting for the effect of continuous light irradiation:

$$\frac{dn_{HS}}{dt} = -n_{HS}(t)K_{HL}(t_r, n_{HS}(t)) + I_0\sigma_a(1 - n_{HS}(t)) \quad , \tag{28}$$

where $I_0\sigma_a$ counts as the LS → HS switching probability rate (I_0 is the light beam intensity and σ_a is the light absorption cross section). Depending on the temperature change rate, two cases can be identified

- *Static LITH*: when the temperature change rate is small as compared to the rate of the other processes involved, so it can be neglected. The metastable states can be identified as fixed points of Eq. (28), which is equivalent to solving, for each value of temperature (t_r), the algebraic equation:

$$K_{HL}(t_r, n_{HS}) = I_0\sigma_a\left(\frac{1}{n_{HS}} - 1\right) \tag{29}$$

Sample results for the metastable states calculations are plotted versus (reduced) temperature in **Figure 15**, for two values of the interaction parameter x. The static LITH phenomenon is apparent in these two examples. As expected, the intermolecular interaction has an important role in LITH, due to the cooperative nature of the relaxation process.

- *Dynamic LITH*: where the temperature change interferes with the other processes and, consequently, the temperature change rate cannot be neglected. Typical hysteretic loops obtained by using Eq. (28) and APC model for K_{HL} are plotted in **Figure 16**, for several values of temperature change rate v_r. The APC model can successfully reproduce the main features of the experimental data reported in LITH properties [93]. By increasing the cooperativity of a SCO system, the LITH width increases accordingly. A similar effect can be obtained "artificially" by increasing the temperature change rate; thus, by increasing the temperature change rate, the system does not have enough time to react at the light effect, so the hysteresis loop is widened.

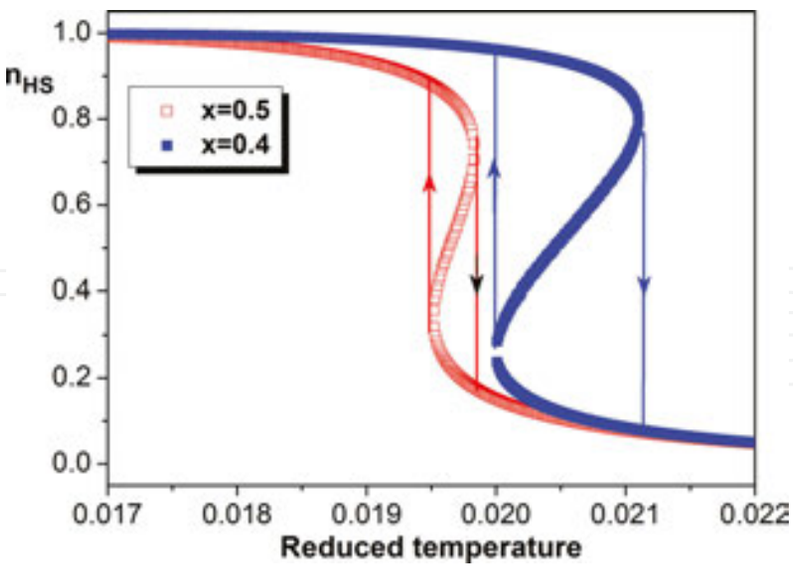

Figure 15. Static LITH for two values of the interaction parameter x. Parameters used in these calculations are $y = 0$, $\delta_0 = 0.6$, $x = 0.1$, $\ln g = 5$, $N = 2000$, $A = 0.8$, $k_\infty = 100$, $I_0\sigma_a = 5 \times 10^{-4}$ s^{-1}.

Although the APC model is able to reproduce a wide range of phenomena, experimentally observed in molecular SCO compounds, it also has some limitations that need to be addressed

by further studies. The first physical limitation of the APC model consists the difficulty of measuring the elastic constants and consequently, the impossibility of measuring the reduced parameter y. This constraint leads to the application of the *trial-and-error* method for identifying a proper value of this parameter needed in a quantitative study instead of a physical identification that would make the model more focused on technical applications. Another important limitation of this model concerns the analysis of the spin-like domains spreading in spin crossover single crystals. Indeed, the spin crossover molecules are considered in APC model as fixed atoms that limit the analysis of the local distortions. These distortions are not only affecting the nearest neighbors but also causing long-range interactions between the system molecules. It is important to notice that some limitations were overcome by newly developed models, such as mechanoelastic model designed by Enachescu et al. [60], where the molecular volume change during the spin transition is taken into account.

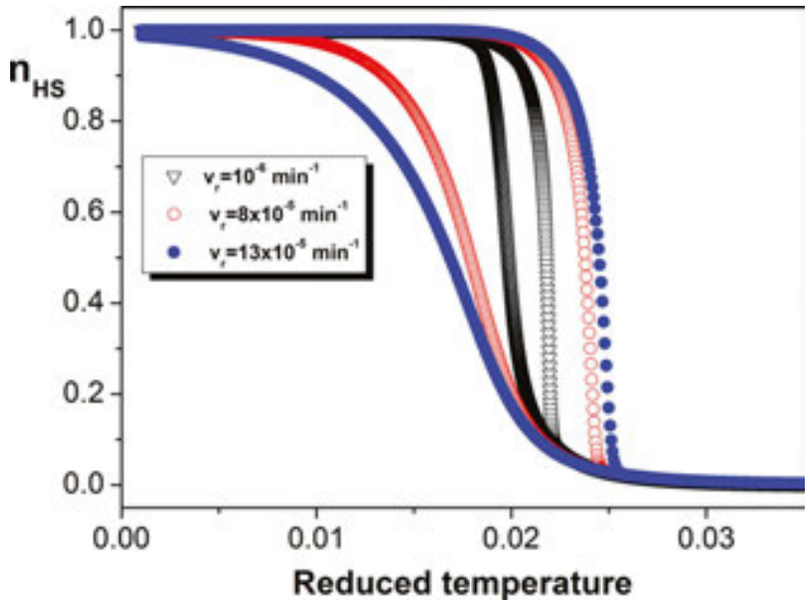

Figure 16. Dynamics LITH for three values of the temperature change rate v_r. Parameters used in the calculations are $x = 0.5$, $y = 0$, $\delta_0 = 0.6$, $x = 0.1$, ln $g = 5$, $N = 2000$, $A = 0.8$, $k_\infty = 100$, $I_0\sigma_a = 5 \times 10^{-4}$ s^{-1}.

3. Conclusions

This chapter provided a general introduction of physical modeling in molecular materials with a special emphasis placed on spin crossover compounds. It covered multiple types of spin crossover compounds and analyzed intermolecular interactions, size effects, thermal behavior, pressure effects, the photoexcitation processes (such as LIESST), relaxation process, and light-induced thermal hysteresis. Numerous illustrations were provided to help the reader in grasping highly abstract concepts, explaining molecular materials behavior, and designing various applications. In this way, we try to support students and young researchers get acquainted to this research area and to facilitate the communication between the mathematical

and physical communities, chemical experimentalists, and engineering practitioners in this field.

Although the models presented here are able to reproduce a wide range of phenomena, experimentally observed in molecular SCO compounds, they also have some limitations that emphasize the need for further research in this area. However, an attentive analysis of the bibliography is needed before deciding to work on a specific problem, since several generalizations have not been explicitly addressed in this short introduction to this novel and dynamic area of research.

Author details

Mihai Dimian[1,2] and Aurelian Rotaru[2*]

*Address all correspondence to: aurelian.rotaru@usm.ro

1 Department of Electrical and Computer Engineering, Howard University, Washington, DC, USA

2 Department of Computers, Electronics and Automation and MANSiD Research Center, Stefan cel Mare University, Suceava, Romania

References

[1] S. Sanvito, *Molecular spintronics*, Chemical Society Reviews, 40 (2011) 3336–3355.

[2] S. Sanvito, *Molecular spintronics: The rise of spinterface science*, Nature Physics, 6 (2010) 562–564.

[3] A. Bousseksou, G. Molnar, L. Salmon, W. Nicolazzi, *Molecular spin crossover phenomenon: recent achievements and prospects*, Chemical Society Reviews, 40 (2011) 3313–3335.

[4] O. Kahn, C.J. Martinez, *Spin-transition polymers: From molecular materials toward memory devices*, Science, 279 (1998) 44–48.

[5] P. Gutlich, *Spin crossover in Iron (II)-complexes*, Structure and Bonding, 44 (1981) 83–195.

[6] S. Decurtins, P. Gutlich, C.P. Kohler, H. Spiering, A. Hauser, *Light induced excited spin state trapping in a transition-metal complex – the hexa-1-propyltetrazole-Iron (II) tetrafluoroborate spin crossover system*, Chemical Physics Letters, 105 (1984) 1–4.

[7] S. Decurtins, P. Gutlich, K.M. Hasselbach, A. Hauser, H. Spiering, *Light induced excited spin state trapping in Iron (II) spin crossover systems – optical spectroscopic and magnetic susceptibility study*, Inorganic Chemistry, 24 (1985) 2174–2178.

[8] A. Hauser, *Reversibility of light-induced excited spin state trapping in the $Fe(ptz)_6(BF_4)_2$ and the $Zn_{1-x}Fe_x(ptz)_6(BF_4)_2$ spin-crossover systems*, Chemical Physics Letters, 124 (1986) 543–548.

[9] C.P. Slichter, H.G. Drickamer, *Pressure-Induced Electronic Changes in Compounds of Iron*, Journal of Chemical Physics, 56 (1972) 2142–2160.

[10] E. Konig, G. Ritter, J. Waigel, H.A. Goodwin, *The effect of pressure on the thermal hysteresis of 1st-order spin transition in bis(1,10-phenanthroline-2carbaldehyde phenylhydrazone) iron (II) complexes*, Journal of Chemical Physics, 83 (1985) 3055–3061.

[11] A. Bousseksou, N. Negre, M. Goiran, L. Salmon, J.P. Tuchagues, M.L. Boillot, K. Boukheddaden, F. Varret, *Dynamic triggering of a spin-transition by a pulsed magnetic field*, European Physical Journal B, 13 (2000) 451–456.

[12] N. Negre, M. Goiran, A. Bousseksou, J. Haasnoot, K. Boukheddaden, Askenazy, F. Varret, *High magnetic field induced spin transition, HMFIST effect, in $[Fe_{0.52}Ni_{0.48}(btr)_2(NCS)_2]H_2O$*, Synthetic Metals, 115 (2000) 289–292.

[13] C. Bartual-Murgui, A. Cerf, C. Thibault, C. Vieu, L. Salmon, G. Molnar, A. Bousseksou, *SERS-active substrates for investigating ultrathin spin-crossover films*, Microelectronic Engineering, 111 (2013) 365–368.

[14] C. Bartual-Murgui, A. Akou, L. Salmon, G. Molnar, C. Thibault, J. Real, A. Bousseksou, *Guest effect on nanopatterned spin-crossover thin films*, Small, 7 (2011) 3385–3391.

[15] X. Bao, H.J. Shepherd, L. Salmon, G. Molnar, M.L. Tong, A. Bousseksou, *The effect of an active guest on the spin crossover phenomenon*, Angewandte Chemie-International Edition, 52 (2013) 1198–1202.

[16] A. Rotaru, F. Varret, E. Codjovi, K. Boukheddaden, J. Linares, A. Stancu, P. Guionneau, J.F. Letard, *Hydrostatic pressure investigation of the spin crossover compound [Fe(PM-BiA)(2)(NCS)(2)] polymorph I using reflectance detection*, Journal of Applied Physics, 106 (2009) 053515.

[17] P. Gutlich, *Thermal and optical switching of bistable iron compounds and possible applications*, Nuclear Instruments & Methods in Physics Research Section B-Beam Interactions with Materials and Atoms, 76 (1993) 387–396.

[18] J. Linares, E. Codjovi, Y. Garcia, *Pressure and temperature spin crossover sensors with optical detection*, Sensors, 12 (2012) 4479–4492.

[19] J. Dai, S. Kanegawa, Z. Li, S. Kang, O. Sato, *A switchable complex ligand exhibiting photoinduced valence tautomerism*, European Journal of Inorganic Chemistry, 2013 (2013) 4150–4153.

[20] A. Vallee, C. Train, C. Roux, *Synthesis and properties of a thermochromic spin crossover Fe-II complex: an undergraduate coordination chemistry laboratory experiment*, Journal of Chemical Education, 90 (2013) 1071–1076.

[21] A. Lapresta-Fernandez, S. Titos-Padilla, J.M. Herrera, A. Salinas-Castillo, E. Colacio, L.F.C. Vallvey, *Photographing the synergy between magnetic and colour properties in spin crossover material Fe(NH(2)trz)(3) (BF4)(2): a temperature sensor perspective*, Chemical Communications, 49 (2013) 288–290.

[22] V. Meded, A. Bagrets, K. Fink, R. Chandrasekar, M. Ruben, F. Evers, A. Bernand-Mantel, J.S. Seldenthuis, A. Beukman, H.S.J. van der Zant, *Electrical control over the Fe(II) spin crossover in a single molecule: Theory and experiment*, Physical Review B, 83 (2011) 245415.

[23] F.-L. Yang, M.-G. Chen, X.-L. Li, J. Tao, R.-B. Huang, L.-S. Zheng, *Two-dimensional iron(II) networks – guest-dependent structures and spin-crossover behaviors*, European Journal of Inorganic Chemistry, 2013 (2013) 4234–4242.

[24] A. Rotaru, I.A. Gural'skiy, G. Molnar, L. Salmon, P. Demont, A. Bousseksou, *Spin state dependence of electrical conductivity of spin crossover materials*, Chemical Communications, 48 (2012) 4163–4165.

[25] A. Rotaru, J. Dugay, R.P. Tan, I.A. Gural'skiy, L. Salmon, P. Demont, J. Carrey, G. Molnar, M. Respaud, A. Bousseksou, *Nano-electromanipulation of spin crossover nanorods: Towards switchable nanoelectronic devices*, Advanced Materials, 25 (2013) 1745–1749.

[26] F. Setifi, C. Charles, S. Houille, F. Thetiot, S. Triki, C.J. Gomez-Garcia, S. Pillet, *Spin crossover (SCO) iron(II) coordination polymer chain: Synthesis, structural and magnetic characterizations of Fe(abpt)(2)(mu-M(CN)(4)) (M = Pt-II and Ni-II)*, Polyhedron, 61 (2013) 242–247.

[27] Y. Qu, *Quantum-chemical investigation of the spin crossover complex Fe(mbpzbpy)(NCS)(2)*, Spectrochimica Acta Part A-Molecular and Biomolecular Spectroscopy, 113 (2013) 427–431.

[28] Y. Li, C.-G. Zhang, L.-Y. Cai, Z.-X. Wang, *Synthesis, crystal structure, Hirshfeld surfaces, and spectral properties of Cu(II) and Co(II) complexes with 3-phenoxymethyl-4-phenyl-5-(2-pyridyl)-1,2,4-triazole*, Journal of Coordination Chemistry, 66 (2013) 3100–3112.

[29] V. Vrdoljak, B. Prugovecki, D. Matkovic-Calogovic, T. Hrenar, R. Dreos, P. Siega, *Three polymorphic forms of a monomeric Mo(VI) complex: Building blocks for two metal-organic supramolecular isomers. Intermolecular interactions and ligand substituent effects*, Crystal Growth & Design, 13 (2013) 3773–3784.

[30] S. Sanvito, *Strategy for detection of electrostatic spin-crossover effect in magnetic molecules*, Physical Review B, 88 (2013) art. no. 054409.

[31] A. Bousseksou, J. Nasser, J. Linares, K. Boukheddaden, F. Varret, *Ising-like model for the 2-step spin-crossover*, Journal of Physics I, 2 (1992) 1381–1403.

[32] M. Sorai, S. Seki, *Phonon coupled cooperative low-Spin 1A1-high spin 5 T2 transition in [Fe(phen)2(NCS)2] and [Fe(phen)2(NCSe)2] crystals*, Journal of Physical Chemistry Solids, 35 (1974) 555–570.

[33] J.A. Nasser, *First order high-spin/low-spin phase transition induced by acoustic-phonons*, European Physical Journal B, 21 (2001) 3–10.

[34] J.A. Nasser, K. Boukheddaden, J. Linares, *Two-step spin conversion and other effects in the atom-phonon coupling model*, European Physical Journal B, 39 (2004) 219–227.

[35] A. Rotaru, J. Linares, *Relaxation and light induced thermal hysteresis (LITH) behaviours in the atom-phonon coupling model for spin crossover compounds*, Journal of Optoelectronics and Advanced Materials, 9 (2007) 2724–2730.

[36] A. Rotaru, J. Linares, E. Codjovi, J. Nasser, A. Stancu, *Size and pressure effects in the atom-phonon coupling model for spin crossover compounds*, Journal of Applied Physics, 103 (2008) 07B908.

[37] A. Rotaru, J. Linares, S. Mordelet, A. Stancu, J. Nasser, *Re-entrance phase and excited metastable electronic spin states in one-dimensional spin crossover compounds explained by atom-phonon coupling model*, Journal of Applied Physics, 106 (2009) 043507.

[38] A. Rotaru, A. Carmona, F. Combaud, J. Linares, A. Stancu, J. Nasser, *Monte Carlo simulations for 1-and 2D spin crossover compounds using the atom-phonon coupling model*, Polyhedron, 28 (2009) 1684–1687.

[39] A. Gindulescu, A. Rotaru, J. Linares, M. Dimian, J. Nasser, *Excited metastables electronic spin states in spin crossover compounds studies by atom-phonon coupling model: Gradual and two-step transition cases*, Journal of Applied Physics, 107 (2010) 09A959.

[40] M.P. Espejo, A. Gindulescu, J. Linares, J. Nasser, M. Dimian, *Phase diagram of two-dimensional spin crossover systems using the atom-phonon coupling model*, Journal of Applied Physics, 109 (2011) art. no. 07B102.

[41] A. Gindulescu, A. Rotaru, J. Linares, M. Dimian, J. Nasser, *Metastable states at low temperature in spin crossover compounds in the framework of the atom-phonon coupling model*, Polyhedron, 30 (2011) 3186–3188.

[42] J. Wajnflasz, *Study of "Low Spin" – "High Spin" transition in octahedral transition ion complexes*, Physica Status Solidi (b), 40 (1970) 537–545.

[43] J. Wajnflasz, R. Pick, *"Low Spin" – "High Spin" transitions in Fe2+ complexes*, Le Journal de Physique Colloques, 32 (1971) C1–91.

[44] R.A. Bari, J. Sivardiere, *Low-spin-high-spin transitions in transition-metal-ion-compounds*, Physical Review B, 5 (1972) 4466–4471.

[45] R. Zimmermann, E. Konig, *Model for high-spin low-spin transitions in solids including effect of lattice vibrations*, Journal of Physics and Chemistry of Solids, 38 (1977) 779–788.

[46] T. Kambara, *Theory of high-spin reversible low-spin transitions in transition-metal compounds induced by the Jahn-Teller effect*, Journal of Chemical Physics, 70 (1979) 4199–4206.

[47] T. Kambara, *The effect of iron concentration on the high-spin reversible low-spin transitions in iron compounds*, Journal of the Physical Society of Japan, 49 (1980) 1806–1811.

[48] T. Kambara, *Theory of high-spin reversible low-spin transitions in transition-metal compounds induced by cooperative molecular distortions and lattice strains*, Journal of Chemical Physics, 74 (1981) 4557–4565.

[49] J. Linares, J. Nasser, K. Boukheddaden, A. Bousseksou, F. Varret, *Monte-Carlo simulations of spin-crossover transitions using the 2-level model. 1: mononuclear single sublattice case*, Journal of Magnetism Magnetic Materials, 140 (1995) 1507–1508.

[50] A.L. Tchougreeff, A.V. Soudackov, I.A. Misurkin, H. Bolvin, O. Kahn, *High-spin low-spin transitions in Fe(II) complexes by effective Hamiltonian method*, Chemical Physics, 193 (1995) 19–26.

[51] H. Bolvin, O. Kahn, *Ising-model for low-spin high-spin transitions in molecular compounds – within and beyond the mean-field approximation*, Chemical Physics, 192 (1995) 295–305.

[52] J. Linares, H. Spiering, F. Varret, *Analytical solution of 1D Ising-like systems modified by weak long range interaction – Application to spin crossover compounds*, European Physical Journal B, 10 (1999) 271–275.

[53] K. Boukheddaden, J. Linares, H. Spiering, F. Varret, *One-dimensional Ising-like systems: An analytical investigation of the static and dynamic properties, applied to spin-crossover relaxation*, European Physical Journal B, 15 (2000) 317–326.

[54] K. Boukheddaden, I. Shteto, B. Hoo, F. Varret, *Dynamical model for spin-crossover solids. I. Relaxation effects in the mean-field approach*, Physical Review B, 62 (2000) 14796–14805.

[55] K. Boukheddaden, *Anharmonic model for phonon-induced first-order transition in 1-D spin-crossover solids*, Progress of Theoretical Physics, 112 (2004) 205–217.

[56] K. Boukheddaden, M. Nishino, S. Miyashita, F. Varret, *Unified theoretical description of the thermodynamical properties of spin crossover with magnetic interactions*, Physical Review B, 72 (2005) 014467.

[57] K. Boukheddaden, S. Miyashita, M. Nishino, *Elastic interaction among transition metals in one-dimensional spin-crossover solids*, Physical Review B, 75 (2007) 094112.

[58] M. Nishino, K. Boukheddaden, Y. Konishi, S. Miyashita, *Simple two-dimensional model for the elastic origin of cooperativity among spin states of spin-crossover complexes*, Physical Review Letters, 98 (2007) art. no. 247203.

[59] A. Dobrinescu, C. Enachescu, A. Stancu, *Ising-like model study of size dependence relaxation in spin crossover complexes*, Journal of Magnetism and Magnetic Materials, 321 (2009) 4132–4138.

[60] C. Enachescu, L. Stoleriu, A. Stancu, A. Hauser, *Model for elastic relaxation phenomena in finite 2D hexagonal molecular lattices*, Physical Review Letters, 102 (2009) 257204.

[61] T.D. Oke, F. Hontinfinde, K. Boukheddaden, *Bethe lattice approach and relaxation dynamics study of spin-crossover materials*, Applied Physics A-Materials Science & Processing, 120 (2015) 309–320.

[62] W. Nicolazzi, S. Pillet, C. Lecomte, *Two-variable anharmonic model for spin-crossover solids: A like-spin domains interpretation*, Physical Review B, 78 (2008) 174401.

[63] G. Felix, W. Nicolazzi, M. Mikolasek, G. Molnar, A. Bousseksou, *Non-extensivity of thermodynamics at the nanoscale in molecular spin crossover materials: A balance between surface and volume*, Physical Chemistry Chemical Physics, 16 (2014) 7358–7367.

[64] I. Gudyma, V. Ivashko, J. Linares, *Diffusionless phase transition with two order parameters in spin-crossover solids*, Journal of Applied Physics, 116 (2014) art. no. 173509.

[65] S. Ohnishi, S. Sugano, *Strain interaction effects on the high-spin low-spin transition of transition-metal compounds*, Journal of Physics C-Solid State Physics, 14 (1981) 39–55.

[66] H. Spiering, E. Meissner, H. Koppen, E.W. Muller, P. Gutlich, *The effect of the lattice expansion on high-spin reversible low-spin transitions*, Chemical Physics, 68 (1982) 65–71.

[67] N. Willenbacher, H. Spiering, *The elastic interaction of high-spin and low-spin complex-molecules in spin-crossover compounds*, Journal of Physics C-Solid State Physics, 21 (1988) 1423–1439.

[68] H. Spiering, N. Willenbacher, *The elastic interaction of high-spin and low-spin complex-molecules in spin-crossover compounds. 2*, Journal of Physics-Condensed Matter, 1 (1989) 10089–10105.

[69] R. Zimmermann, *A model for high-spin low-spin transitions with an interpretation of thermal hysteresis effects*, Journal of Physics and Chemistry of Solids, 44 (1983) 151–158.

[70] P. Gutlich, H. Koppen, R. Link, H.G. Steinhauser, *Interpretation of high-spin reversible low-spin transition in iron(II) complexes. 1. Phenomenological thermodynamic model*, Journal of Chemical Physics, 70 (1979) 3977–3983.

[71] A. Bousseksou, H. Constantmachado, F. Varret, *A simple Ising-like model for spin-conversion including molecular vibrations*, Journal De Physique I, 5 (1995) 747–760.

[72] A. Gîndulescu, A. Rotaru, J. Linares, M. Dimian, J. Nasser, *Analysis of phase transitions in spin-crossover compounds by using atom – phonon coupling model*, Journal of Physics: Conference Series, 268 (2011) 012007.

[73] A. Rotaru, A. Graur, G.-M. Rotaru, J. Linares, Y. Garcia, *Influence of intermolecular interactions and size effect on LITH-FORC diagram in 1D spin crossover compounds*, Journal of Optoelectronics and Advanced Materials, 14 (2012) 529–536.

[74] F. Varret, S.A. Salunke, K. Boukheddaden, A. Bousseksou, E. Codjovi, C. Enachescu, J. Linares, *The Ising-like model applied to switchable inorganic solids: discussion of the static properties*, Comptes Rendus Chimie, 6 (2003) 385–393.

[75] K. Boukheddaden, J. Linares, E. Codjovi, F. Varret, V. Niel, J.A. Real, *Dynamical Ising-like model for the two-step spin-crossover systems*, Journal of Applied Physics, 93 (2003) 7103–7105.

[76] D. Chiruta, J. Linares, P.R. Dahoo, M. Dimian, *Analysis of long-range interaction effects on phase transitions in two-step spin-crossover chains by using Ising-type systems and Monte Carlo entropic sampling technique*, Journal of Applied Physics, 112 (2012) 074906.

[77] D. Chiruta, J. Linares, Y. Garcia, M. Dimian, P.R. Dahoo, *Analysis of multi-step transitions in spin crossover nanochains*, Physica B: Condensed Matter 434 (2014) 134–138.

[78] D. Chiruta, J. Linares, Y. Garcia, P.R. Dahoo, M. Dimian, *Analysis of the hysteretic behaviour of 3D spin crossover compounds by using an Ising-like model*, European Journal of Inorganic Chemistry, 21 (2013) 3601–3608.

[79] D. Chiruta, J. Linares, M. Dimian, Y. Alayli, Y. Garcia, *Role of edge atoms in the hysteretic behaviour of 3D spin crossover nanoparticles revealed by an Ising-like model*, European Journal of Inorganic Chemistry, 29 (2013) 5086–5093.

[80] A. Rotaru, *Theoretical and experimental study of the effect of pressure and size on bistable compounds: thermal behavior and relaxation study*, PhD Thesis, GEMaC, Universite de Versailles et Saint Quentin en Yvellines, 2009.

[81] Z. Yu, C. Li, X.Z. You, H. Spiering, P. Gutlich, Y.F. Hsia, *Debye-Waller factor in the spin crossover complex Fe(ppi)(2)(NCS)(2)*, Materials Chemistry and Physics, 48 (1997) 150–155.

[82] M.M. Dirtu, Y. Garcia, M. Nica, A. Rotaru, J. Linares, F. Varret, *Iron(II) spin transition 1,2,4-triazole chain compounds with novel inorganic fluorinated counteranions*, Polyhedron, 26 (2007) 2259–2263.

[83] J. Jung, H. Spiering, Z. Yu, P. Gutlich, *The Debye-Waller factor in spincrossover molecular crystals – a Mossbauer study on* $[Fe_xZn_{1-x}(ptz)(6)](BF_4)(2)$, Hyperfine Interactions, 95 (1995) 107–128.

[84] J. Jung, G. Schmitt, L. Wiehl, A. Hauser, K. Knorr, H. Spiering, P. Gutlich, *The cooperative spin transition in* $[Fe_xZn_{1-x}(ptz)(6)](BF_4)(2)$. *2. Structural properties and calculation of the elastic interaction*, Zeitschrift Fur Physik B-Condensed Matter, 100 (1996) 523–534.

[85] J.M. Yeomans, *Statistical Mechanics of Phase Transitions*, Oxford University Press: Oxford, 1992.

[86] R. Balian, *From Microphysics to Macrophysics. Methods and Applications of Statistical Physics*, Springer: Berlin, 1991.

[87] C.-M. Jureschi, I. Rusu, E. Codjovi, J. Linares, Y. Garcia, A. Rotaru, *Thermo- and piezochromic properties of* $[Fe(hyptrz)]A2 \cdot H_2O$ *spin crossover 1D coordination polymer: Towards spin crossover based temperature and pressure sensors*, Physica B: Condensed Matter, 449 (2014) 47–51.

[88] A. Hauser, P. Gutlich, H. Spiering, *High-spin low-spin relaxations kinetics and cooperative effects in the hexakis(1-propyltetrazole)iron bis(tetrafluoroborate) and* $[Zn_{1-x}Fe_x(ptz)_6](BF_4)_2$*(ptz = 1-propyltetrazole) spin crossover systems*, Inorganic Chemistry, 25 (1986) 4245–4248.

[89] A. Hauser, *Intersystem crossing in Fe(II) coordination-compounds*, Coordination Chemistry Reviews, 111 (1991) 275–290.

[90] A. Hauser, *Cooperative effects on the HS–LS relaxation in the [Fe(ptz)6](BF4)2 spin-crossover system*, Chemical Physics Letters, 192 (1992) 65–70.

[91] C. Enachescu, *Phd Thesis*, *Contributions to the study of instability induced by light in photomagnetic inorganic solids*, LMOV, Universite de Versailles et Saint Quentin en Yvelines, 2003.

[92] J.F. Letard, P. Guionneau, L. Rabardel, J.A.K. Howard, A.E. Goeta, D. Chasseau, O. Kahn, *Structural, magnetic, and photomagnetic studies of a mononuclear iron(II) derivative exhibiting an exceptionally abrupt spin transition. Light-induced thermal hysteresis phenomenon.* Inorganic Chemistry, 37 (1998) 4432–4441.

[93] C. Enachescu, H.C. Machado, N. Menendez, E. Codjovi, J. Linares, F. Varret, A. Stancu, *Static and light induced hysteresis in spin-crossover compounds: experimental data and application of Preisach-type models*, Physica B-Condensed Matter, 306 (2001) 155–160.

IntechOpen